



Intrinsic thermal conductivity and its anisotropy of wurtzite InN

Jinlong Ma, Wu Li, and Xiaobing Luo

Citation: [Applied Physics Letters](#) **105**, 082103 (2014); doi: 10.1063/1.4893882

View online: <http://dx.doi.org/10.1063/1.4893882>

View Table of Contents: <http://scitation.aip.org/content/aip/journal/apl/105/8?ver=pdfcov>

Published by the [AIP Publishing](#)

Articles you may be interested in

[Thermal conductivity of bulk and nanowire InAs, AlN, and BeO polymorphs from first principles](#)

J. Appl. Phys. **114**, 183505 (2013); 10.1063/1.4827419

[Theoretical calculation of the vibrational and thermal properties of wurtzite InN-GaN multiple quantum well superlattice](#)

J. Appl. Phys. **113**, 164304 (2013); 10.1063/1.4802683

[Suppression of thermal conductivity in In_xGa_{1-x}N alloys by nanometer-scale disorder](#)

Appl. Phys. Lett. **102**, 121906 (2013); 10.1063/1.4798838

[Carrier and phonon dynamics of wurtzite InN nanorods](#)

Appl. Phys. Lett. **94**, 071911 (2009); 10.1063/1.3086888

[Calculated optical properties of wurtzite InN](#)

J. Appl. Phys. **101**, 033123 (2007); 10.1063/1.2435802



AIP | Journal of
Applied Physics

Journal of Applied Physics is pleased to
announce **André Anders** as its new Editor-in-Chief

Intrinsic thermal conductivity and its anisotropy of wurtzite InN

 Jinlong Ma,¹ Wu Li,^{2,a)} and Xiaobing Luo^{1,b)}
¹State Key Laboratory of Coal Combustion, School of Energy and Power Engineering, Huazhong University of Science and Technology, Wuhan 430074, China

²Scientific Computing & Modelling NV, De Boelelaan 1083, 1081 HV Amsterdam, The Netherlands

(Received 26 June 2014; accepted 12 August 2014; published online 25 August 2014)

Despite wurtzite InN being a widely used semiconductor, its intrinsic thermal conductivity (κ) is still little known. In this work, the κ of wurtzite InN is studied from first principles. The calculated room temperature κ is $130 \text{ Wm}^{-1}\text{K}^{-1}$ and $145 \text{ Wm}^{-1}\text{K}^{-1}$ for the in-plane and out-of-plane direction, respectively, showing an anisotropy of about 11%. The anisotropy increases with decreasing temperature, and it reaches 20% at 100 K. The evident anisotropy is contrast to the conventionally used isotropic assumption, and is explained by performing comprehensive velocity analysis. We also calculate the cumulative κ as a function of mean free path, which can help understand the size dependence of κ in the non-bulk forms. The obtained cumulative κ is in good agreement with the experimental κ of InN films with thicknesses between 0.5 and $2.1 \mu\text{m}$, and shows the size effect can persist up to $10 \mu\text{m}$ thickness at room temperature. © 2014 AIP Publishing LLC.

[<http://dx.doi.org/10.1063/1.4893882>]

Wurtzite InN has attracted considerable attention for its extremely narrow electronic band gap 0.7 eV (Ref. 1) and low electron effective mass $0.05 m_e$.² Its alloy with wurtzite GaN, which has emission range from the ultraviolet to the near-infrared region,³ has been widely used as quantum wells material in the optoelectronic devices, such as light emitting diodes^{4–6} and laser diodes.^{7–9} Its high absorption coefficient ($\sim 10^5 \text{ cm}^{-1}$) and robustness also make it suitable for solar cell applications.^{10–12} In addition, InN is expected to be used for high electron mobility transistors^{13–15} due to the high mobility and high saturation velocity¹⁶ coming from the low effective mass. Despite the fact, many researches on the electronic carrier transport properties of InN have been done,^{17–23} the investigation on the thermal transport properties, which is critical for the heat dissipation, is still relatively little. The first reported thermal conductivity (κ) of InN grown by nitrogen microwave plasma chemical vapor deposition is $45 \text{ Wm}^{-1}\text{K}^{-1}$.²⁴ Later measurement on high-quality InN films with thicknesses between 0.5 and $2.1 \mu\text{m}$ gives a κ of $120 \text{ Wm}^{-1}\text{K}^{-1}$.²⁵ The knowledge for the intrinsic κ of bulk single crystals is still lacking.

Over the past several years, *ab initio* calculation of κ has been developed by combining the first principles techniques to obtain interatomic force constants (IFCs) with Boltzmann transport equation (BTE). So far, this method has been applied to many systems,^{26–45} showing good agreement with available experimental data. Some of the authors and coworkers have recently published an open-source code ShengBTE,⁴⁶ which allows to calculate the third-order IFCs using a real-space finite-difference approach^{39,46} along with third-party *ab initio* packages and eventually κ using a locally adaptive algorithm to treat the Gaussian function approximation for the Dirac delta function.^{30,46} In this work, we use this *ab initio* method to investigate the intrinsic κ of wurtzite InN as well as its anisotropy. The contribution of

mean free paths (MFPs) is also studied, which is used to understand the κ measured from InN films.

The density-functional-theory (DFT) calculations are performed for wurtzite InN. The structure is first optimized for the unit cell and, then, the harmonic and the third-order anharmonic IFCs are calculated by using the real-space supercell approach. We refer the reader for details of the DFT calculations to Ref. 46. The Phonopy package⁴⁷ is used to obtain the harmonic IFCs, and the ShengBTE package⁴⁶ is used to obtain the third-order anharmonic IFCs and solve the BTE. The calculated lattice constants are $a = 3.5067 \text{ \AA}$ and $c = 5.6680 \text{ \AA}$, which are in good agreement with the experimentally determined values, $a = 3.5340 \text{ \AA}$ and $c = 5.7088 \text{ \AA}$.⁴⁸ The phonon dispersion calculated from the harmonic IFCs along several high-symmetry directions for wurtzite InN is shown in Fig. 1. For comparison, the experimental data of Raman scattering and x-ray scattering are also plotted. It can be seen that both

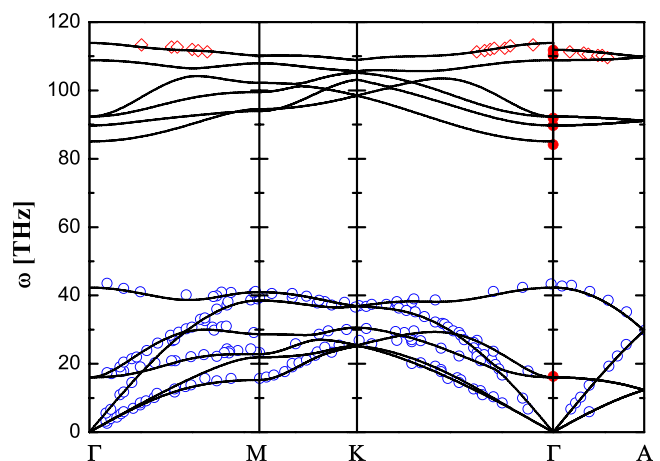


FIG. 1. Calculated phonon dispersions for wurtzite InN along several high-symmetry directions. The solid lines are the results of *ab initio* calculation. The solid circles are the Raman data from Ref. 49. The hollow diamonds show resonant Raman scattering data from Ref. 50. The hollow circles correspond to the x-ray scattering spectroscopies data from Ref. 48.

^{a)}Electronic mail: wu.li.phys2011@gmail.com

^{b)}Electronic mail: luoxb@hust.edu.cn

the acoustic and optical phonons have excellent agreement with the experimental data.

In wurtzite structure, the out-of-plane direction is defined as along the c -axis and the in-plane direction is perpendicular to c -axis. The calculated κ of wurtzite InN is plotted in Fig. 2. At room temperature, the κ is $130 \text{ Wm}^{-1} \text{ K}^{-1}$ and $145 \text{ Wm}^{-1} \text{ K}^{-1}$ for the in-plane and out-of-plane direction, respectively, giving an anisotropy of about 11%. As temperature increases, the anisotropy reduces monotonically, with 20% at 100 K to 9% at 500 K. The obvious anisotropy of κ is contrary to previous isotropic assumption.²⁵ In the conventionally isotropic assumption, the main argument is that the average acoustic phonon velocity in the out-of-plane direction differs from that of in-plane by only 2%. The velocities of out-of-plane and in-plane direction are, respectively, extracted from $\Gamma - A$ and $\Gamma - M$ direction at small wave vector for longitudinal acoustic (LA) and transverse acoustic (TA) branches. Specifically, the average acoustic velocities ($v_s^{-1} = [2v_{TA}^{-1} + v_{LA}^{-1}]/3$) in the $\Gamma - A$ and $\Gamma - M$ direction are, respectively, $3.44 \times 10^3 \text{ m/s}$ and $3.39 \times 10^3 \text{ m/s}$ from experiment,⁴⁸ while they are $3.25 \times 10^3 \text{ m/s}$ and $3.24 \times 10^3 \text{ m/s}$ from our *ab initio* calculation. Both the experiment and calculation show that the difference is really below 2%. However, it is too rude to use the average velocity obtained in this simple way as the average velocity of out-of-plane and in-plane direction, as only the modes at small wave vector along one specific direction are included.

Thus, in order to understand the anisotropy, the κ as a function of frequency at room temperature is plotted in Fig. 3(a). The contribution to the κ from the phonons with a given frequency ω can be obtained as $\kappa_{\omega,\alpha} = \frac{1}{k_B T^2 N V} f_0 (1 + f_0) (\hbar\omega)^2 \sum_{\lambda} v_{\lambda,\alpha}^2 \tau_{\lambda} \delta(\omega - \omega_{\lambda})$,³⁴ where N is the number of uniform \mathbf{q} sampling in the Brillouin zone, V is the volume of the unit cell, f_0 is the Bose-Einstein distribution function, τ_{λ} is the relaxation time of phonon mode λ , and $v_{\lambda,\alpha}$ is the velocity along the α direction. Here, δ function is approximated with Gaussian function $\delta(\omega - \omega_{\lambda}) \approx \frac{1}{\sqrt{2\pi}\sigma} e^{-(\omega - \omega_{\lambda})^2 / 2\sigma^2}$, where σ is adaptive broadening parameter depending on the mode group velocity.⁴⁶ It can be seen that the distribution of κ_{ω} also shows evident anisotropy. As κ_{ω} is related to the square

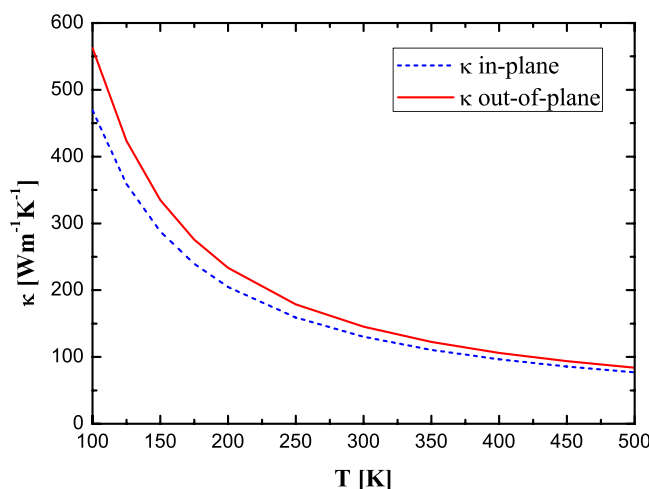


FIG. 2. Calculated thermal conductivity as a function of temperature for wurtzite InN.

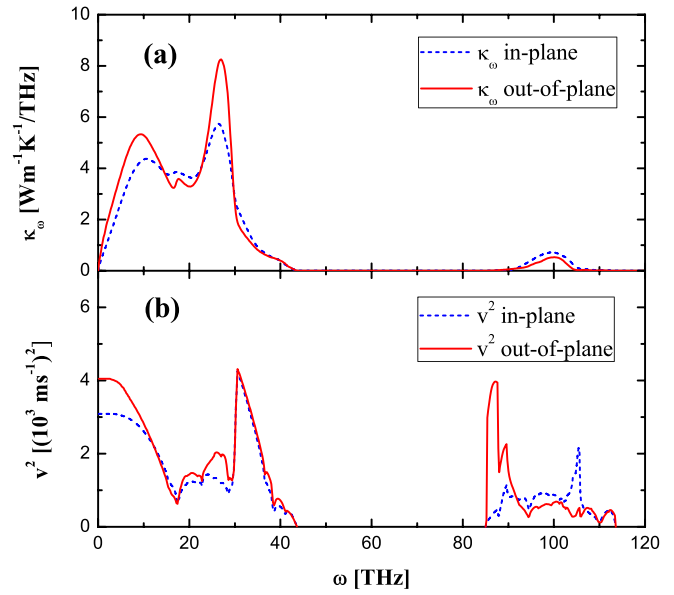


FIG. 3. (a) The contribution to the thermal conductivity from different frequencies for wurtzite InN at room temperature. (b) The average of the square of group velocities along different directions.

of velocity (v^2), the anisotropy of v^2 can reflect the anisotropy of κ_{ω} to some extent though the anisotropy of them is not necessarily the same. Different from the average velocity analysis resulting in the isotropic argument, we average the square of velocity for the in-plane and out-of-plane direction by including all phonon modes. The average velocity, calculated with $v_{\alpha}^2(\omega) = \frac{\sum_{\lambda} v_{\lambda,\alpha}^2 \delta(\omega - \omega_{\lambda})}{\sum_{\lambda} \delta(\omega - \omega_{\lambda})}$, is plotted in Fig. 3(b). As v_{α}^2 is converged down to 3.5 THz with the \mathbf{q} grid used in our calculation, the average velocities below 3.5 THz are replaced with those for 3.5 THz, considering the linear dispersion at low frequencies. For low frequency acoustic phonons, the linear dispersion can be well described as $\omega_p(\mathbf{q}, \theta, \phi) = \mathbf{v}_p(\theta, \phi) \cdot \hat{\mathbf{r}} \mathbf{q}$ by using spherical coordinates and $\hat{\mathbf{r}} \equiv (\sin \theta \cos \phi, \sin \theta \sin \phi, \cos \theta)$.³⁴ After some algebra, the low frequency average velocity is calculated with

$$v_{\alpha}^2(\omega) = \frac{\sum_p \int \int v_{p,\alpha}^2 [\mathbf{v}_p(\theta, \phi) \cdot \hat{\mathbf{r}}]^{-3} \sin \theta d\theta d\phi}{\sum_p \int \int [\mathbf{v}_p(\theta, \phi) \cdot \hat{\mathbf{r}}]^{-3} \sin \theta d\theta d\phi}, \quad (1)$$

where p denotes the three acoustic branches. The results show the v_{α}^2 at the low frequency limit agree with those for 3.5 THz within 5%. It can be seen that at low frequency limit, the difference of the v_{α}^2 is about 30%, with $4.05 (\times 10^3 \text{ m/s})^2$ for the out-of-plane direction and $3.09 (\times 10^3 \text{ m/s})^2$ for the in-plane direction. This large difference is strongly in contrast to the comparison of the velocities along certain high symmetry directions. Therefore, wurtzite InN can have evident anisotropy in κ . The anisotropy increases with decreasing temperature, as low frequency phonons with stronger anisotropy contribute more to κ . We also notice the anisotropy for InN is larger than other wurtzite compounds such as InAs, AlN, and BeO.³⁴

Since InN is always used in the form of thin films, it is instructive to examine the distribution of phonon MFP for the understanding of the size effect on the thermal transport. The cumulative κ as a function of MFP at room temperature is plotted in Fig. 4. The definition of the scalar MFP for mode λ is $\Lambda_{\lambda} = \mathbf{F}_{\lambda} \cdot \mathbf{v}_{\lambda} / |\mathbf{v}_{\lambda}|$ from ShengBTE, where \mathbf{F}_{λ} is

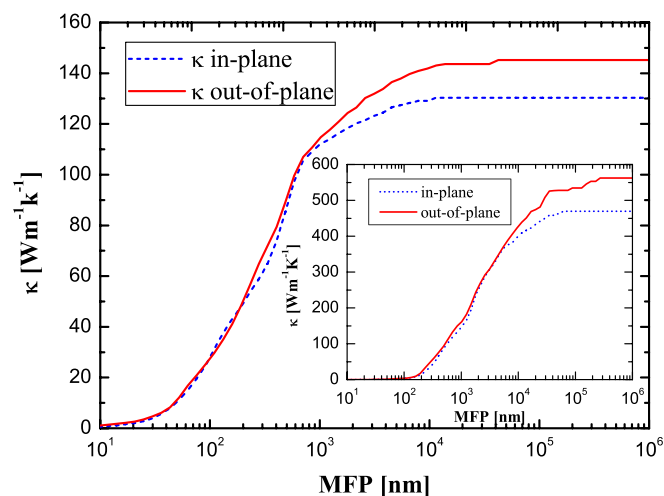


FIG. 4. The cumulative thermal conductivity as a function of mean free path at room temperature. Inset: the cumulative thermal conductivity as a function of mean free path at 100 K.

the mean free displacement obtained by solving BTE.⁴⁶ It shows that there is almost no phonons with MFP less than 10 nm in wurtzite InN at room temperature, and the κ is mainly contributed by the phonons with MFP less than 10 μm , about 100% in the in-plane direction and 98% in the out-of-plane direction. The cumulative κ for the in-plane direction is almost the same with that of out-of-plane when the MFP is less than 1 μm . This reveals that the larger κ for the out-of-plane direction is associated with phonons with large MFPs, which have low frequencies. This agrees with the analysis for κ_{ω} . Along the c -axis of wurtzite InN, the cumulative κ at 0.5 μm and 2.1 μm is 90 $\text{Wm}^{-1}\text{K}^{-1}$ and 126 $\text{Wm}^{-1}\text{K}^{-1}$, respectively, showing good agreement with recently experimental value, 120 $\text{Wm}^{-1}\text{K}^{-1}$, for the thin films with thicknesses 0.5–2.1 μm .²⁵ The phonons with MFP above 2.1 μm contribute about 8% and 13% κ for the in-plane and out-of-plane direction, respectively. The cumulative κ versus MFP at 100 K is also plotted in the inset of Fig. 4. For wurtzite InN at 100 K, phonons with MFP above 2.1 μm contribute about 45% κ for the in-plane direction and 53% κ for the out-of-plane direction.

In summary, the intrinsic κ of wurtzite InN is investigated with the *ab initio* calculation in this work. The room temperature κ is 130 $\text{Wm}^{-1}\text{K}^{-1}$ and 145 $\text{Wm}^{-1}\text{K}^{-1}$ for the in-plane and out-of-plane directions, respectively. In contrast to the isotropic argument, we find evident anisotropy for κ , decreasing from 20% at 100 K to 9% at 500 K. The mean free path distribution well explains the measured κ for films, and shows the size effect can persist up to 10 μm thickness for room temperature and up to larger size at lower temperatures.

We thank Dr. Natalio Mingo for helpful discussions on this work and assistance of the relevant IFCs calculation. J. L. Ma and X. B. Luo acknowledge supports from National Nature Science Foundation of China (No. 51376070) and in part by the Major State Basic Research Development Program of China (No. 2011CB013105).

¹J. Wu, W. Walukiewicz, K. M. Yu, J. W. Ager, E. E. Haller, H. Lu, W. J. Schaff, Y. Saito, and Y. Nanishi, *Appl. Phys. Lett.* **80**, 3967 (2002).

- ²S. P. Fu and Y. F. Chen, *Appl. Phys. Lett.* **85**, 1523 (2004).
- ³A. G. Bhuiyan, A. Hashimoto, and A. Yamamoto, *J. Appl. Phys.* **94**, 2779 (2003).
- ⁴S.-N. Lee, H. S. Paek, H. Kim, T. Jang, and Y. Park, *Appl. Phys. Lett.* **92**, 081107 (2008).
- ⁵X. H. Wang, L. W. Guo, H. Q. Jia, Z. G. Xing, Y. Wang, X. J. Pei, J. M. Zhou, and H. Chen, *Appl. Phys. Lett.* **94**, 111913 (2009).
- ⁶C. B. Soh, W. Liu, S. J. Chua, S. S. Ang, R. J. N. Tan, and S. Y. Chow, *J. Appl. Phys.* **108**, 093501 (2010).
- ⁷S. Nakamura, M. Senoh, S. Nagahama, N. Iwasa, T. Yamada, T. Matsushita, Y. Sugimoto, and H. Kiyoku, *Appl. Phys. Lett.* **69**, 4056 (1996).
- ⁸T. Akasaka, T. Nishida, T. Makimoto, and N. Kobayashi, *Appl. Phys. Lett.* **84**, 4104 (2004).
- ⁹S.-H. Yen and Y.-K. Kuo, *J. Appl. Phys.* **103**, 103115 (2008).
- ¹⁰X. Zheng, R.-H. Horng, D.-S. Wu, M.-T. Chu, W.-Y. Liao, M.-H. Wu, R.-M. Lin, and Y.-C. Lu, *Appl. Phys. Lett.* **93**, 261108 (2008).
- ¹¹E. Matioli, C. Neufeld, M. Iza, S. C. Cruz, A. A. Al-Heji, X. Chen, R. M. Farrell, S. Keller, S. DenBaars, U. Mishra, S. Nakamura, J. Speck, and C. Weisbuch, *Appl. Phys. Lett.* **98**, 021102 (2011).
- ¹²S.-B. Choi, J.-P. Shim, D.-M. Kim, H.-I. Jeong, Y.-D. Jho, Y.-H. Song, and D.-S. Lee, *Appl. Phys. Lett.* **103**, 033901 (2013).
- ¹³W. Chikhaoui, J.-M. Bluet, M.-A. Poisson, N. Sarazin, C. Dua, and C. Bru-Chevallier, *Appl. Phys. Lett.* **96**, 072107 (2010).
- ¹⁴S. Ganguly, A. Konar, Z. Hu, H. Xing, and D. Jena, *Appl. Phys. Lett.* **101**, 253519 (2012).
- ¹⁵A. Sasikumar, A. R. Arehart, S. Martin-Horcajo, M. F. Romero, Y. Pei, D. Brown, F. Recht, M. A. di Forte-Poisson, F. Calle, M. J. Tadjer, S. Keller, S. P. DenBaars, U. K. Mishra, and S. A. Ringel, *Appl. Phys. Lett.* **103**, 033509 (2013).
- ¹⁶W. A. Hadi, P. K. Guram, M. S. Shur, and S. K. O'Leary, *J. Appl. Phys.* **113**, 113709 (2013).
- ¹⁷V. Lebedev, V. Cimalla, T. Baumann, O. Ambacher, F. M. Morales, J. G. Lozano, and D. Gonzalez, *J. Appl. Phys.* **100**, 094903 (2006).
- ¹⁸V. M. Polyakov and F. Schwierz, *Appl. Phys. Lett.* **88**, 032101 (2006).
- ¹⁹R. E. Jones, S. X. Li, E. E. Haller, H. C. M. van Genuchten, K. M. Yu, J. W. Ager, Z. Liliental-Weber, W. Walukiewicz, H. Lu, and W. J. Schaff, *Appl. Phys. Lett.* **90**, 162103 (2007).
- ²⁰X.-G. Yu and X.-G. Liang, *J. Appl. Phys.* **103**, 043707 (2008).
- ²¹X. Wang, S.-B. Che, Y. Ishitani, and A. Yoshikawa, *Appl. Phys. Lett.* **92**, 132108 (2008).
- ²²N. Ma, X. Q. Wang, S. T. Liu, G. Chen, J. H. Pan, L. Feng, F. J. Xu, N. Tang, and B. Shen, *Appl. Phys. Lett.* **98**, 192114 (2011).
- ²³S. Wang, H. Liu, B. Gao, and H. Cai, *Appl. Phys. Lett.* **100**, 142105 (2012).
- ²⁴S. Krukowski, A. Witek, J. Adamczyk, J. Jun, M. Bockowski, I. Grzegory, B. Lucznik, G. Nowak, M. Wrblewski, A. Presz, S. Gierlotka, S. Stelmach, B. Palosz, S. Porowski, and P. Zinn, *J. Phys. Chem. Solids* **59**, 289 (1998).
- ²⁵A. X. Levander, T. Tong, K. M. Yu, J. Suh, D. Fu, R. Zhang, H. Lu, W. J. Schaff, O. Dubon, W. Walukiewicz, D. G. Cahill, and J. Wu, *Appl. Phys. Lett.* **98**, 012108 (2011).
- ²⁶D. A. Broido, M. Malorny, G. Birner, N. Mingo, and D. A. Stewart, *Appl. Phys. Lett.* **91**, 231922 (2007).
- ²⁷A. Ward and D. A. Broido, *Phys. Rev. B* **81**, 085205 (2010).
- ²⁸K. Esfarjani, G. Chen, and H. T. Stokes, *Phys. Rev. B* **84**, 085204 (2011).
- ²⁹A. Ward, D. A. Broido, D. A. Stewart, and G. Deinzer, *Phys. Rev. B* **80**, 125203 (2009).
- ³⁰W. Li, N. Mingo, L. Lindsay, D. A. Broido, D. A. Stewart, and N. A. Katcho, *Phys. Rev. B* **85**, 195436 (2012).
- ³¹D. A. Broido, L. Lindsay, and A. Ward, *Phys. Rev. B* **86**, 115203 (2012).
- ³²X. Tang and J. Dong, *Proc. Natl. Acad. Sci. U.S.A.* **107**, 4539 (2010).
- ³³J. Garg, N. Bonini, B. Kozinsky, and N. Marzari, *Phys. Rev. Lett.* **106**, 045901 (2011).
- ³⁴W. Li and N. Mingo, *J. Appl. Phys.* **114**, 054307 (2013).
- ³⁵J. Carrete, W. Li, N. Mingo, S. Wang, and S. Curtarolo, *Phys. Rev. X* **4**, 011019 (2014).
- ³⁶Z. Tian, J. Garg, K. Esfarjani, T. Shiga, J. Shiomi, and G. Chen, *Phys. Rev. B* **85**, 184303 (2012).
- ³⁷L. Lindsay, D. A. Broido, and T. L. Reinecke, *Phys. Rev. Lett.* **109**, 095901 (2012).
- ³⁸L. Lindsay, D. A. Broido, and T. L. Reinecke, *Phys. Rev. B* **87**, 165201 (2013).

- ³⁹W. Li, L. Lindsay, D. A. Broido, D. A. Stewart, and N. Mingo, *Phys. Rev. B* **86**, 174307 (2012).
- ⁴⁰W. Li and N. Mingo, *J. Appl. Phys.* **114**, 183505 (2013).
- ⁴¹H. Dekura, T. Tsuchiya, and J. Tsuchiya, *Phys. Rev. Lett.* **110**, 025904 (2013).
- ⁴²J. W. L. Pang, W. J. L. Buyers, A. Chernatynskiy, M. D. Lumsden, B. C. Larson, and S. R. Phillpot, *Phys. Rev. Lett.* **110**, 157401 (2013).
- ⁴³L. Lindsay, D. A. Broido, and T. L. Reinecke, *Phys. Rev. Lett.* **111**, 025901 (2013).
- ⁴⁴S. Lee, K. Esfarjani, J. Mendoza, M. S. Dresselhaus, and G. Chen, *Phys. Rev. B* **89**, 085206 (2014).
- ⁴⁵W. Li and N. Mingo, *Phys. Rev. B* **89**, 184304 (2014).
- ⁴⁶W. Li, J. Carrete, N. A. Katcho, and N. Mingo, *Comput. Phys. Commun.* **185**, 1747 (2014).
- ⁴⁷A. Togo, F. Oba, and I. Tanaka, *Phys. Rev. B* **78**, 134106 (2008).
- ⁴⁸J. Serrano, A. Bosak, M. Krisch, F. J. Manjón, A. H. Romero, N. Garro, X. Wang, A. Yoshikawa, and M. Kuball, *Phys. Rev. Lett.* **106**, 205501 (2011).
- ⁴⁹V. Y. Davydov, V. V. Emtsev, I. N. Goncharuk, A. N. Smirnov, V. D. Petrikov, V. V. Mamutin, V. A. Vekshin, S. V. Ivanov, M. B. Smirnov, and T. Inushima, *Appl. Phys. Lett.* **75**, 3297 (1999).
- ⁵⁰V. Davydov, A. Klochikhin, A. Smirnov, I. Strashkova, A. Krylov, H. Lu, W. Schaff, H.-M. Lee, Y.-L. Hong, and S. Gwo, *Semiconductors* **44**, 161 (2010).